Research Square

Preprints are preliminary reports that have not undergone peer review.
They should not be considered conclusive, used to inform clinical practice,
or referenced by the media as validated information.

Transcriptomic associations of a pre-specified 468-gene redox and xenobiotic-metabolism panel across five neurological disorders, with a published-variant inventory

Mark E. McCaulley

mark@siriusneuroscience.com

Sirius Neuroscience, LLC https://orcid.org/0000-0003-2059-622X

Research Article

Keywords: Alzheimer disease, Parkinson disease, transcriptomics, redox, meta-analysis, xenobiotic metabolism

Posted Date: November 20th, 2026

DOI: https://doi.org/10.21203/rs.3.rs-11800620/v1

License: This work is licensed under a Creative Commons Attribution 4.0 International License.
Read Full License

Additional Declarations: The authors declare potential competing interests as follows: The author is sole inventor on a provisional patent application covering panel-based research scoring methods that use the locked 468-gene list reported here. The application did not determine gene membership, the high-confidence rule, or the results. GVI, DDI, and IDRS are unvalidated research constructs. Academic reuse of the deposited panel and code does not require a license from the author. The author declares no other competing interests.

Transcriptomic associations of a pre-specified 468-gene redox and xenobiotic-metabolism panel across five neurological disorders, with a published-variant inventory

Short title: Disease-specific 468-gene panel patterns in five neurological disorders

Mark E. McCaulley, M.D.

Sirius Neuroscience, LLC, Steamboat Springs, Colorado 80487, USA

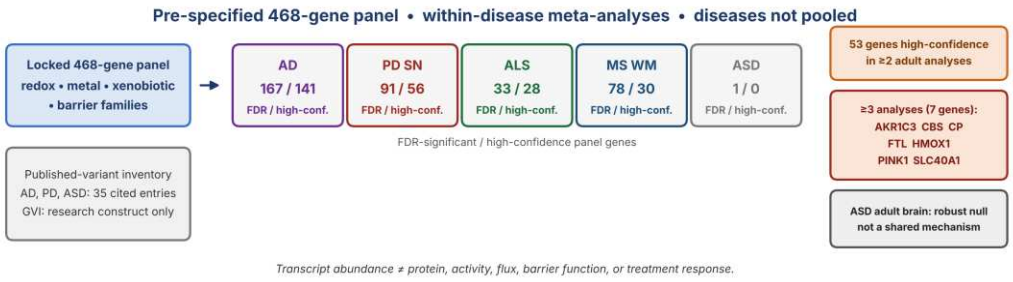
ORCID: 0000-0003-2059-622X | Correspondence: mark@siriusneuroscience.com

Keywords: Alzheimer disease; Parkinson disease; transcriptomics; redox; meta-analysis; xenobiotic metabolism

ABSTRACT

Five neurological disorders—Alzheimer's disease (AD), autism spectrum disorder (ASD), Parkinson's disease (PD), multiple sclerosis (MS), and amyotrophic lateral sclerosis (ALS)—have distinct clinical and pathological features. I performed independent within-disease random-effects meta-analyses of public transcriptomic cohorts using an immutable 468-gene redox, metal-homeostasis, xenobiotic-metabolism, and barrier panel, and separately inventoried published variants in panel genes for AD, PD and ASD. AD brain, ALS spinal cord/motor neuron, and MS white matter showed disease-specific patterns; in bulk PD substantia nigra two external cohorts supported the high-confidence set in direction and rank but not in per-gene significance. Across the four adult neurodegenerative analyses, 53 genes met the locked high-confidence rule in at least two analyses (Online Resource 3). Seven genes—AKR1C3, CBS, CP, FTL, HMOX1, PINK1, and SLC40A1—met that rule in at least three; CBS was up in AD and PD and down in MS, so the rule does not imply uniform direction or a shared mechanism. HMOX1 was positive in several adult analyses; GSS and GSR transcripts were lower in AD and PD. Adult ASD postmortem brain was a robust FDR null (1 of 392 genes analyzable in at least two cohorts; that gene did not meet the high-confidence rule). Cell-type datasets in MS and PD supply compartment context only. A competitive gene-label permutation test did not show that the 468-gene panel out-enriched power-matched random sets. Inference is gene-level within the locked list, not list-level enrichment. Published variants in panel genes are inventoried for AD, PD and ASD (35 cited entries in the companion manuscripts); they are context for proposed research constructs, not clinical risk scores.

GRAPHICAL ABSTRACT



Graphical abstract. Independent within-disease meta-analyses of a locked 468-gene panel. Counts are FDR-significant / high-confidence genes. Diseases were not statistically pooled. GVI and related constructs are research organizers only.

INTRODUCTION

Five neurological disorders—AD, ASD, PD, MS, and ALS—have distinct clinical, pathological, tissue, and temporal features. This study evaluates whether selected pre-specified genes in redox, metal-homeostasis, xenobiotic-metabolism, and barrier-associated families show reproducible transcriptomic associations within disease, and whether published variants in panel genes can be inventoried transparently, disease by disease. Individual-disease studies have previously reported related observations in each of these disorders, including glutathione-related findings in AD [1], glutathione S-transferase genotype associations in ASD [2], nigral glutathione loss in PD [3], SOD1 mutations in familial ALS [4], and the clinical use of the NRF2-activating agent dimethyl fumarate in MS [5]. These observations were made in separate literatures using different designs and are cited here as background rather than as evidence of a shared mechanism.

The study compares independent within-disease random-effects transcriptomic meta-analyses using an immutable, pre-specified 468-gene panel, and separately inventories published variants in panel genes for AD, PD and ASD. The aim is not to establish a common upstream mechanism or to perform a new genome-wide association study, but to identify partial gene-level transcriptomic overlap, disease-specific divergence, and an auditable record of published genetic associations in selected iron/redox, glutathione-related, xenobiotic-metabolism, and neurovascular-associated genes.

I present this comparison alongside five companion single-disease manuscripts that are posted elsewhere (AD, ASD, PD, MS, and ALS companions). Those companions use the same locked panel and high-confidence rule; they are disease-resolved analyses, not a second cross-disease pooling. The 468-gene panel represents xenobiotic-metabolism, antioxidant-defense, metal-homeostasis, and barrier-associated functional families. It was assembled by functional-family enumeration, not data-driven feature selection, and builds on the previously published foundation signature [6]. The panel was not derived from the XenoReg detoxification and physiological-barrier gene set of Santos et al. [7]; overlap with that 519-gene set was inspected after the freeze and was not used to add or remove genes. Pre-specified, rule-based filters were applied:

pseudogenes and ambiguous symbols were removed, and only genes passing a group-blind detection threshold within a dataset were analyzed. Genes were not added or removed on the basis of case-versus-control association. The panel, given in full in Online Resource 2, is immutable. Across AD, ASD, PD, MS, and ALS, the analysis compares disease-specific transcriptomic associations and directional replication while preserving the tissue, developmental, cohort, platform, and cell-type limitations that shape each result.

MATERIALS AND METHODS

Statistical note on DDI values. Per-dataset DDI values cited in the disease-specific companion analyses derive from the locked definition: panel-restricted Benjamini–Hochberg adjusted $P < 0.05$ and absolute log2 fold-change at least 0.5. These values are descriptive. Random-effects 468-panel meta-analyses are the primary inferential results. Large language models (Grok, xAI; Claude, Anthropic; and Perplexity) were used to assist literature synthesis, pipeline construction, editorial refinement, and critical review of claims; the author reviewed all output and takes responsibility for the content. No generative tool is an author.

The standardized 468-gene panel includes xenobiotic-metabolism, antioxidant-defense, metal-homeostasis, and barrier-associated functional families and was assembled by functional-family enumeration. The locked high-confidence rule is restated in Online Resource 1. Official panel tiers and the excluded-symbol list are given in Online Resource 2. A 40-gene sensitivity layer and a 12-gene placental/sex-steroid module are reported separately from CORE. Public GEO transcriptomic datasets spanning AD, ASD, PD, MS, and ALS were screened; locked primary within-disease meta-analyses used the accessions listed in Online Resource 1 and in the Zenodo deposit (concept DOI https://doi.org/10.5281/zenodo.22178093). Additional series are supporting or model contrasts and are not added to those primary k counts. RNA-seq cohorts were analyzed with PyDESeq2 and microarray cohorts with limma; p-values were Benjamini–Hochberg FDR-adjusted. Separately, published variants in panel genes were inventoried for AD, PD and ASD from the companion manuscripts (Table 1); odds ratios were taken from the cited source studies and were not re-estimated. GVI, DDI, and IDRS are proposed research constructs only. Their formulas, uncalibrated scaling, dataset accessions, the rule for variants entering a GVI, and limitations are provided in Online Resource 1 and are not inferential claims of this article. In that note DDI is expressed as a percent (0–100) of measurable panel genes in a given dataset; the $|\log2FC| \geq 0.5$ floor applies to DDI only. They are not clinical risk scores, diagnostic tools, prognostic tools, treatment-selection tools, or treatment-response predictors. Competitive versus self-contained tests were distinguished a priori. Primary inference is per-gene within-disease random-effects meta-analysis under the locked high-confidence rule (self-contained at the gene). List-level competitive inference used gene-label permutation of power-matched random sets of size 468 from the measurable background. CAMERA (correlation-adjusted mean rank) [32] is the parametric competitive counterpart; it was not used to define, revise, or interpret the locked panel.

Competitive inference in this article is the gene-label permutation. Subsets reported in this article are partitions of the locked 468-gene panel and are not a revised invention list.

RESULTS

Cross-Disease Gene-Level Patterns and Divergence

Independent random-effects meta-analyses were performed within each disease, with pooled log2 fold-changes reported throughout (Fig. 1). Where a gene was represented by more than one microarray probe, the probe with the smallest P value was used in the primary analysis, with two documented exceptions: the Alzheimer cohorts GSE5281 and GSE48350 contributed the mean of the probe-level estimates, and the ALS exon-array cohorts GSE56500 and GSE18920 were averaged within transcript cluster because smallest-P selection made 58% of genes nominally significant against 12–14% of individual probesets. Significance-based probe selection depends on the outcome and can inflate cohort-level evidence; probe-averaging sensitivity analyses are reported in each companion manuscript. High-confidence genes were defined as FDR < 0.05, measured in at least three cohorts, direction-concordant in at least 70% of cohorts, and independently significant in at least two cohorts. The rule is therefore applicable only where primary $k \geq 3$ (AD, PD substantia nigra, ALS, MS white matter). Genes measured in only two cohorts, including most of the adult ASD set, cannot meet it. The rule does not impose an I^2 cap. Median I^2 among high-confidence genes differed by disease (AD 79.3%; ALS 56.7%; PD 16.4%; MS white matter 0%), so AD and ALS pooled effects should be read as directionally reproducible under high between-cohort heterogeneity, not as homogeneous effects.

Within-disease significant-gene counts are summarized in Fig. 2. In AD, 458 of 468 panel genes were meta-analyzable across six brain cohorts, and 167 reached FDR < 0.05, including 141 high-confidence genes. In PD, four substantia-nigra cohorts yielded 91 FDR-significant genes, including 56 high-confidence genes; frontal cortex was reported separately. In ALS, seven cohorts spanning laser-capture-microdissected motor neurons and bulk spinal cord yielded 33 FDR-significant genes among 449 analysable panel genes, including 28 high-confidence genes, with compartment stratification retained. These ALS figures come from a donor-resolved analysis (one value per donor; exon arrays averaged within transcript cluster); an earlier locked analysis of the same seven cohorts, which pooled all tissues of GSE153960 and both tissue compartments of GSE18920 and selected exon-array probesets by significance, gave 26 and 22 and is superseded. In MS, the white-matter primary meta-analysis pooled three white-matter cohorts and yielded 78 FDR-significant genes, including 30 high-confidence genes; the gray-matter cohort was reported separately. The adult ASD postmortem-brain meta-analysis was a robust FDR null: among 392 panel genes meta-analyzable in at least two cohorts, 1 reached FDR < 0.05. That gene is MAFK (pooled log2FC −0.34; $I^2 = 0\%$; independently significant in 1 of 3 cohorts). MAFK did not meet the high-confidence rule and is not interpreted as an adult-ASD signature.

The primary analyses were conducted independently within disease and were not statistically pooled across diseases. Across the four adult neurodegenerative disease analyses, 53 genes met the locked high-confidence criterion in at least two disease-specific meta-analyses. That intersection is descriptive; no cross-disease p-value is attached. The 53 genes are listed in Online Resource 3, which uses the donor-resolved ALS analysis. The CROSS-DISEASE sheet of the Zenodo workbook was built on the superseded ALS analysis and lists a different 53, with NFE2L2, PPARG, SLC30A5 and SP3 in place of BACH1, CYP51A1, HMOX2 and SIRT1. Seven genes—AKR1C3, CBS, CP, FTL, HMOX1, PINK1, and SLC40A1—met the high-confidence criterion in at least three disease-specific analyses, and none met it in all four. CBS was high-confidence up in AD and PD and high-confidence down in MS white matter; PINK1 was high-confidence down in AD, PD and ALS; CP and FTL were high-confidence up in PD, ALS and MS white matter. This criterion reflects reproducibility of pre-specified gene-level patterns within diseases; it does not imply uniform effect direction, tissue localization, cell type, or biological role across diseases, nor does it indicate a shared mechanism.

Disease-specific associations were substantial. CYP26A1 was downregulated in AD and MS white matter but was neutral in PD and ALS. APOE transcript was strongly positive in ALS, and AQP1 and AQP4 were positive and high-confidence in the ALS analysis. In MS, white-matter and gray-matter results differed for selected iron/redox genes, supporting tissue-stratified interpretation rather than a single MS effect. HMOX1 illustrates the need for contextual interpretation: it showed positive pooled effects across several adult neurodegenerative disease analyses, while its relevant tissue, cellular context, and potential biological role differed among PD, MS, and ALS. In ALS, bulk spinal-cord and laser-capture-microdissected motor-neuron cohorts differed for several glial-associated genes. These distinctions are retained rather than reconciled into a single cross-disease effect.

Glutathione-related transcriptomic findings were disease- and tissue-dependent. GSS and GSR transcripts were downregulated in AD and PD. These observations concern transcript abundance and do not establish glutathione flux, enzyme activity, or GSH/GSSG status. In ALS, the regional distribution of panel hits differed between spinal cord and occipital cortex. In MS, GPX4 findings were lesion- and compartment-contextual and should be interpreted alongside oligodendrocyte composition and potential per-cell transcriptional differences. Published STING–GPX4 biochemistry is extra-CNS experimental context [13], not a measured ferroptosis event in the MS white-matter meta-analysis.

Barrier-associated genes showed heterogeneous, compartment-specific associations. CLDN5, CGN, CLDN11, and related genes should be interpreted in the relevant disease, tissue, and cell-composition context [8, 9]; transcript levels do not directly establish barrier function. Published paraoxonase findings [10–12] and selected CNS cGAS–STING, ICAM1, and PECAM1 reports [14–17] are not interpreted here as universal cross-disease signals.

The adult ASD postmortem-brain meta-analysis was a robust null in the sampled cohorts. This result distinguishes the adult-brain analysis from developmental-model findings, but does not exclude developmental, maternal, genetic, environmental, or cell-context-specific mechanisms. CYP26-family findings in ASD developmental models are therefore described as developmental-model retinoic-acid-handling associations rather than as an adult-brain or universal disease mechanism.

Published Genetic-Variant Inventory

In addition to the within-disease transcriptomic meta-analyses, published variants in panel genes were inventoried for three of the five diseases (Table 1). The inventory is not a new association study, and no variant was genotyped in the analysed cohorts. It comprises 35 entries, each itemised with its source in a companion manuscript: 10 in Alzheimer's disease (the Alzheimer companion, its Table 6), 10 in Parkinson's disease (the Parkinson companion, its Table 5) and 15 in autism (the autism companion, its Table 8). The entries are heterogeneous: main-effect associations, gene–environment interactions, maternal-genotype findings and findings with non-disease outcomes. Only some carry an odds ratio that could enter a GVI; in Alzheimer's disease, 4 of the 10 do. The multiple sclerosis and ALS companions are transcriptomic analyses and contain no variant inventory. The rule that only variants with an established odds ratio enter a GVI, and the ancestry caveats that apply, are given in Online Resource 1.

The Genetic Vulnerability Index (GVI), Detoxification Dysregulation Index (DDI), and Integrated Detoxification Risk Score (IDRS) are proposed research frameworks for organizing those published genetic associations together with tissue-level transcriptomic measures. Full definitions, the percent form of DDI, the uncalibrated IDRS = GVI + DDI/10 scaling, a worked illustration, the rule for variants entering a GVI, and nonclinical-use limitations are given only in Online Resource 1. These constructs are not diagnostic, prognostic, treatment-selection, treatment-response, or patient-level clinical risk tools, and they are not inferential claims of this article.

Where a dataset-level DDI is cited, it is the percent of measurable panel genes meeting the locked definition used throughout (panel-restricted Benjamini–Hochberg adjusted $P < 0.05$ and absolute log2 fold-change at least 0.5). In the four held-out AD cohorts the same whole-panel DDI was compared with a matched Monte-Carlo null; that comparison is a list-level negative control, not a second DDI definition. Thresholds are provisional. Published genetic odds ratios that could enter a GVI differ by ancestry, exposure context, population, and study design and do not capture epistasis or all gene–environment interactions.

Disease-Specific Associations

Supporting model contrast (not in the locked primary k). Mutation-specific AD transcriptomic patterns. The two PSEN1 mutations examined showed different panel signatures despite both showing substantial panel dysregulation. In A79V, GCLC, GCLM, GSS, metallothionein-related transcripts, TJP1, and APOE showed selected differences relative to the isogenic comparison. In

L150P, EPHX2 was upregulated. These differences demonstrate that aggregate DDI values can obscure mutation-specific transcriptomic patterns. They generate mechanistic hypotheses but do not establish pathway failure, causal mediation, or treatment selection.

The APOE-cysteine-glutathione formulation remains a testable hypothesis. APOE isoforms differ in cysteine content, and glutathione-related transcripts differed in selected AD datasets. This observation does not establish baseline glutathione capacity in APOE carriers or identify a supplementation-responsive subgroup.

NRF2/KEAP1-related transcriptomic context. NRF2/KEAP1-related transcripts and antioxidant-response genes provide disease- and compartment-specific mechanistic context [18–23]. Transcript abundance does not establish NRF2 protein activity, pathway flux, or a treatment-responsive state. Published intervention studies [22, 23] are background evidence, not evidence that the present analysis identifies a therapeutic classifier.

Metallothionein patterns differed by disease, tissue, and cell type. AD brain meta-analysis showed selected metallothionein upregulation, while mutation models differed. PD substantia-nigra cell-type data suggested isoform- and cell-context-specific patterns [24]. MS datasets supported astrocyte-associated MT1A context in lesions [25]. These observations should not be treated as a uniform metallothionein response across diseases.

ALDH1A1 in PD. ALDH1A1 was a strong substantia-nigra spatial marker and was downregulated in dopaminergic neurons and protoplasmic astrocytes in the cited cell-type-resolved analysis [26]. This localization provides mechanistic context for a PD-specific DOPAL-related hypothesis; it does not prove a causal pathway in human PD. Published aldehyde-dehydrogenase knockout models provide external experimental support for the DOPAL hypothesis [27, 28].

CYP26 and ASD developmental-model retinoic-acid associations. CYP26A1, CYP26B1, and CYP26C1 were recurrently dysregulated in selected ASD developmental-model comparisons, with direction varying by model and developmental context. These findings were distinct from the robust adult ASD postmortem-brain null and support further study of developmental-model retinoic-acid handling. They do not establish a universal developmental mechanism or a clinical intervention strategy.

ALS anatomical specificity and early model-associated GPX4 change. In the NYGC ALS Consortium cohort, panel hit rates were higher in cervical and lumbar spinal cord than in occipital cortex, supporting an anatomical distribution of transcriptomic association. Separately, as a supporting model contrast (not in the locked primary k), GPX4 was downregulated before symptom onset in a SOD1-G93A laser-capture motor-neuron model (GSE10953; three animals per group, uncorrected P values). Temporal precedence and published perturbation evidence strengthen mechanistic hypotheses but do not establish causality. Selected genes, including AQP4,

APOE transcript, NQO1, CP, and CLDN5, showed directional concordance across multiple ALS datasets; interpretation remains dependent on bulk versus motor-neuron compartment.

Cell-Type-Resolved Context

Cell-type-resolved datasets in MS and PD provide useful context for selected bulk-tissue signals, but they are not uniform across diseases and do not alone establish causal pathway engagement. In MS, available single-nucleus analyses [25] quantify cellular composition and support interpretation of bulk findings; direct pseudobulk differential-expression analysis within cell types remains necessary. GPX4-associated findings are consistent with both oligodendrocyte depletion and possible per-cell transcriptional differences. HMOX1 and MT1A observations are interpreted in lesion stage and cell-composition context.

In PD, substantia-nigra cell-type data localized selected signals to microglial, astrocytic, neuronal, and other cellular populations [26, 29]. These results support interpretation of HMOX1, ALDH1A1, GPX4, SLC7A11, HSPA1A, and cGAS-STING observations but should be distinguished from bulk-tissue replication. Comparable cell-type resolution is not available for the AD analyses. ALS evidence combines bulk tissue, laser-capture microdissection, and molecular-subtype localization rather than uniform single-cell disease-control analysis.

External Replication of Pre-Specified Signatures

Independent external cohorts were used to compare disease-specific panel-gene log2 fold-changes with the corresponding discovery meta-analysis, with high-confidence genes specified as the primary readout and gene-label permutation as the baseline. Directional signature replication was observed in AD cortex that is predominantly temporal (GSE15222; $r = 0.83$, 95% directional concordance, $n = 86$ genes) and MS CNS tissue (GSE123496; $r = 0.73$, 83%, $n = 30$ genes); both correlations exceeded their gene-label permutation baselines (95th-percentile $|r| = 0.21$ and 0.35; permutation $P = 0.0002$ for each). Against the 28 donor-resolved ALS high-confidence genes, direction replicated in whole blood (GSE112676; 20 of 26 measurable genes concordant, 77%, exact binomial $P = 0.0094$) but not in motor/frontal cortex (GSE124439; 19 of 28, 68%, $P = 0.087$), and the magnitude correlation did not exceed its permutation baseline in either cohort ($r = 0.24$ and 0.29; permutation $P = 0.24$ and 0.14). ALS figures reported for these two cohorts in an earlier version of this analysis rested on incomplete data exports and on the superseded ALS gene set. In ASD, the independent analysis was null, consistent with the adult-brain robust-null result. In bulk PD substantia nigra, two external cohorts that contributed nothing to the locked meta-analysis supported the high-confidence set in direction and rank (GSE20292: 41 of 54 genes concordant, exact binomial $P = 0.0002$, Spearman $\rho = 0.61$; GSE168496: 38 of 55, $P = 0.006$, $\rho = 0.43$), but not in per-gene significance. The genes higher in PD replicated in the array cohort but at little better than chance in the RNA-sequencing cohort, an asymmetry consistent with a composition-sensitive component of the bulk-tissue signal that

neuronal loss and gliosis can produce. Both external cohorts are small, and donor-level independence of GSE20292 from the locked cohort GSE20141 cannot be verified from the deposited records. An earlier statement that bulk PD substantia nigra did not replicate externally rested on an incomplete data export and is superseded. As a further out-of-sample list-level control, the frozen panel was applied to four Alzheimer-disease cohorts that are absent from the locked primary accession list (GSE1297, GSE36980, GSE29378, GSE118553; 253 cases, 188 controls). In those cohorts the whole-panel DDI did not exceed its matched Monte-Carlo null (fold-enrichment 0.52–1.20). Per-sample panel-score discrimination is not an inferential claim of this article.

These results concern directional reproducibility of selected pre-specified high-confidence genes. They do not demonstrate preferential enrichment of the full 468-gene panel over the transcriptome. In the terminology of Goeman and Bühlmann [31], the high-confidence rule is a self-contained, gene-level filter: it asks whether a named panel transcript replicates across independent cohorts of one disease. A competitive gene-label permutation (power-matched random 468-gene sets drawn from the measurable background, same high-confidence rule) did not show that the full panel out-enriched those random sets. That negative result is the list-level competitive finding of this article. The locked 468 genes comprise CORE redox/metal/xenobiotic/barrier genes (n = 394), CORE cGAS–STING (n = 12), CORE ferroptosis/iron/NRF2 (n = 10), a 40-gene sensitivity layer, and a 12-gene placental/sex-steroid module (394 + 12 + 10 + 40 + 12 = 468). Those named subsets are partitions of the same frozen list, not a revised panel. Tier names follow the panel file, except that the tier labelled “ASD-maternal module” in the file is called the placental/sex-steroid module here. Blood cohorts assess peripheral rather than brain compartments.

DISCUSSION

Using an immutable, pre-specified 468-gene panel of redox-, metal-homeostasis-, xenobiotic-metabolism-, and barrier-associated genes, this study identified partial gene-level overlap together with substantial disease-specific divergence in transcriptomic associations across AD, ASD, PD, MS, and ALS. In parallel, published variants in panel genes were inventoried for AD, PD and ASD as an auditable record of published associations. The primary transcriptomic analyses were conducted independently within each disease and retained important differences in tissue source, cellular composition, lesion context, disease stage, and platform. The genetic-variant component likewise remains disease-stratified: variant inventories are not pooled across disorders, and published odds ratios are not re-estimated here. Across the four adult neurodegenerative disease analyses, selected transcripts showed reproducible directional patterns in more than one disease-specific meta-analysis, but neither directionality nor biological context was uniform across disorders. These findings support focused mechanistic investigation of iron/redox, glutathione-related, xenobiotic-metabolism, and neurovascular-associated signals rather than a single universal mechanism.

NRF2/KEAP1-related transcripts and antioxidant-response genes may provide disease- and compartment-specific mechanistic context. Transcript abundance does not establish NRF2 protein activity, pathway flux, or a treatment-responsive state. Published intervention studies [22, 23] are relevant background evidence, but the present study neither tests interventions nor identifies a therapeutic classifier.

Published intervention literature (including dimethyl fumarate in MS) provides external biological context for selected transcript patterns. That literature is not evidence that the present analysis nominates agents, selects patients, or predicts treatment response.

The ASD maternal-axis and developmental hypotheses remain distinct from the adult postmortem-brain transcriptomic null. Published epidemiological and intervention literature can motivate prospective research, but the present cross-disease transcriptomic analysis does not establish maternal causal mechanisms, preventive effects, or individualized intervention strategies. Maternal half-sibling recurrence data are one such published source [30].

The study used random-effects models with per-gene heterogeneity, a locked high-confidence rule, compartment stratification, and polarity checks. These procedures support auditable within-disease inference but cannot eliminate the limitations of heterogeneous public cohorts or establish biological causality.

LIMITATIONS

Results are reported in two locked arms. The primary arm is within-disease random-effects meta-analysis of public GEO transcriptomic cohorts for a pre-specified 468-gene panel (AD, PD, ALS, MS, ASD analyzed separately; diseases were never statistically pooled). The second arm inventories published variants in panel genes for AD, PD and ASD from the companion manuscripts; odds ratios were taken from the cited source studies and were not re-estimated. No new tissue was collected and no new GWAS was performed. Gene-level high-confidence transcriptomic calls are the primary inferential claim. List-level competitive permutation of the 468-gene set was negative and is not reported as enrichment.

This study synthesizes transcriptomic analyses across heterogeneous public datasets that differ in tissue source, disease stage, cellular composition, platform, sample size, and preprocessing history. The primary analyses were conducted within disease and were not statistically pooled across diseases. Although the same pre-specified 468-gene panel and core random-effects framework were used, a future harmonized reanalysis using consistent preprocessing where raw data are available would strengthen comparability. Tissue and compartment stratification remain essential: for example, MS white matter and gray matter showed divergent iron/redox patterns, and ALS bulk spinal cord and laser-capture-microdissected motor-neuron cohorts differed for several glial-associated genes.

Transcript abundance does not directly establish protein abundance, enzymatic activity, cellular flux, barrier function, or causal pathway engagement. This limitation is especially relevant for NRF2/KEAP1 signaling, antioxidant enzymes, and barrier-associated genes, whose transcript levels may reflect cell composition, injury response, disease stage, or compensatory regulation. Cell-type analyses in MS and PD provide useful context but are not equivalent across diseases. In MS, the available single-nucleus analysis quantifies cellular composition and supports interpretation of bulk findings; direct pseudobulk differential-expression analysis within cell types remains necessary. Comparable cell-type resolution is not yet available for the AD analyses, and ALS evidence combines bulk tissue, laser-capture microdissection, and molecular-subtype localization rather than uniform single-cell disease-control analysis.

The cross-disease claims are limited to reproducibility of pre-specified gene-level directional patterns. A competitive permutation analysis did not show that the full 468-gene panel out-enriched power-matched random gene sets. The supported inference is self-contained, disease-specific reproducibility of selected pre-specified genes—not preferential whole-panel enrichment over the transcriptome. External replication was directional and was most informative for pre-specified high-confidence genes; effect sizes across all panel genes were more variable.

The adult ASD postmortem-brain meta-analysis was a robust null in the sampled cohorts, but that result does not exclude developmental, maternal, genetic, environmental, or cell-context-specific mechanisms. Likewise, external support in bulk PD substantia nigra was limited to direction and rank, in two small cohorts, with an asymmetry between higher and lower genes that neuronal loss and cellular composition may produce; additional replication in appropriate tissue and cell-type-resolved designs is needed. In ALS, direction replicated in whole blood but not in cortex, and magnitude replicated in neither.

The DDI is a descriptive tissue-level measure with provisional thresholds. The GVI aggregates published disease-associated odds ratios that vary across studies, ancestry groups, exposure contexts, and populations and do not capture epistasis or all gene–environment interactions. The IDRS combines these quantities using an uncalibrated scaling choice. Accordingly, GVI, DDI, and IDRS are proposed research frameworks; they are not diagnostic, prognostic, treatment-selection, or treatment-response tools. Their evaluation requires prospective, multi-ancestry studies with clinically relevant outcomes and accessible, biologically appropriate tissues.

Finally, no primary wet-laboratory experiments were performed. Temporal precedence in the SOD1-G93A model, published perturbation datasets, external directional replication, and cross-modal evidence strengthen mechanistic hypotheses but do not establish causality. Direct perturbation studies, protein/activity measurements, and prospective human cohorts are required to test causal relationships and therapeutic relevance.

CONCLUSION

Using a pre-specified 468-gene panel of redox-, metal-homeostasis-, xenobiotic-metabolism-, and barrier-associated genes, independent within-disease random-effects transcriptomic meta-analyses, and inventories of published genetic variants for AD, PD and ASD, this study identifies both reproducible overlap and substantial divergence in gene-expression patterns across AD, ASD, PD, MS, and ALS, together with an auditable record of published genetic associations. Across the four adult neurodegenerative disease analyses, 53 genes met the locked high-confidence criterion in at least two disease-specific meta-analyses. Seven genes—AKR1C3, CBS, CP, FTL, HMOX1, PINK1, and SLC40A1—met that criterion in at least three; CBS was up in AD and PD and down in MS, so direction and biological context were not uniform across diseases.

The results support further study of disease-specific iron/redox, glutathione-related, xenobiotic-metabolism, and neurovascular associations. HMOX1 illustrates the value of this approach: it showed positive pooled effects across several adult neurodegenerative disease analyses, while its relevant tissue, cellular context, and potential biological role differed among PD, MS, and ALS. The ASD adult postmortem-brain analysis was a robust null, distinguishing the adult-brain result from developmental-model findings without excluding developmental or maternal mechanisms.

Cell-type-resolved data in MS and PD provide mechanistic context for selected transcriptomic signals, and external analyses support directional reproducibility of pre-specified signatures in independent AD, MS and PD cohorts and in ALS whole blood, but not in ALS cortex. These findings generate testable mechanistic hypotheses but do not establish causal pathways, universal disease mechanisms, or treatment-response predictions. The GVI, DDI, and IDRS are proposed research frameworks requiring prospective, multi-ancestry validation before any clinical application.

Taken together, the work provides an auditable framework for comparing pre-specified panel transcripts and published genetic variants across neurological diseases while retaining the tissue, cohort, platform, cell-type, developmental, ancestry, and study-design limitations that shape each disease-specific result.

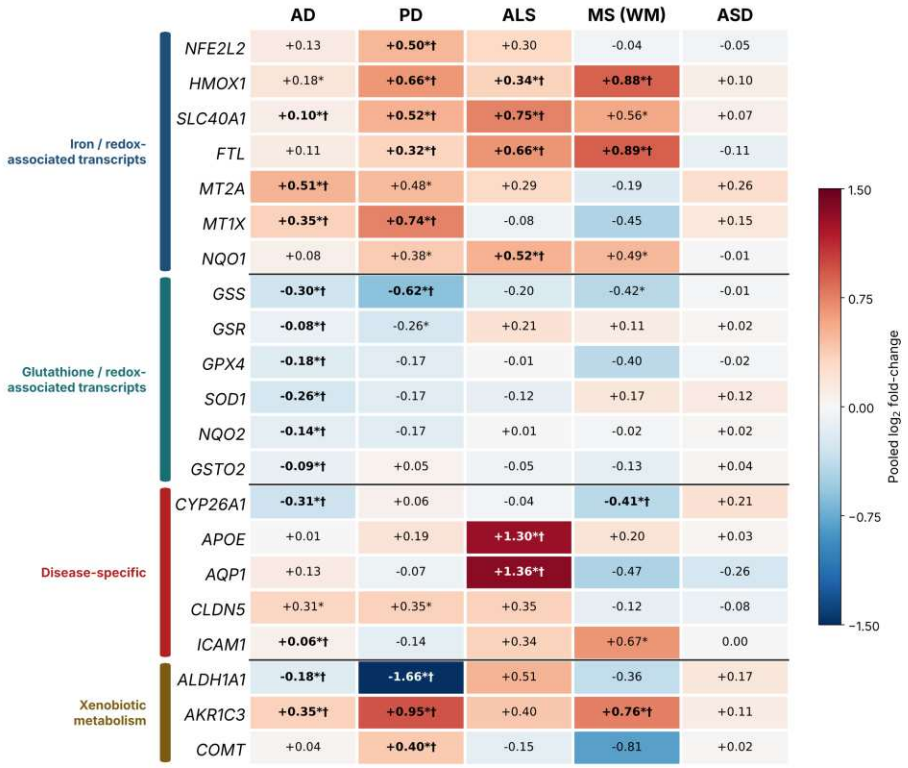
ACKNOWLEDGMENTS

The author acknowledges the GEO investigators who deposited the datasets analyzed in this work, including the New York Genome Center ALS Consortium for GSE153960; the MS Atlas investigators for GSE138614; Macnair et al. for the MS snRNA-seq atlas data; Ma et al. and Al-Dalahmah et al. for PD substantia-nigra data; and the AddNeuroMed consortium investigators. The disease-resolved companion manuscripts thank additional dataset generators. This study used only publicly available, de-identified gene-expression data; no new human-subjects research was conducted and institutional review board approval was not required. Use of AI-assisted tools is declared in the section immediately preceding the references.

FIGURES AND TABLES

Fig. 1. Selected within-disease panel-gene associations

Pooled log_2 fold-change for 21 pre-specified panel genes from independent within-disease meta-analyses



Cell value = pooled log_2 fold-change. * FDR < 0.05 *† high-confidence (bold). MS = white-matter meta-analysis; ASD = adult postmortem brain (robust null). ALS = donor-resolved seven-cohort meta-analysis. Functional groupings organize display only and do not imply uniform pathway activation or cross-disease statistical pooling. Heterogeneity (I^2) is reported in the disease-specific companion manuscripts.

Fig. 1. Selected disease-specific transcriptomic patterns among pre-specified panel genes. Random-effects pooled effect sizes for selected pre-specified redox-, metal-, xenobiotic-metabolism-, and barrier-associated genes across independent within-disease meta-analyses. Functional groupings provide biological organization and do not imply uniform pathway activation, causal engagement, comparable cellular origin, or cross-disease statistical pooling. Each cell gives pooled log2 fold-change with within-disease significance markers. The MS column is the white-matter primary meta-analysis; the gray-matter cohort is reported separately. The ALS column is the donor-resolved seven-cohort meta-analysis. The ASD adult postmortem-brain analysis is a robust null. Cross-disease displays summarize selected disease-specific patterns and should be interpreted in the context of tissue, cellular composition, cohort, and disease stage.

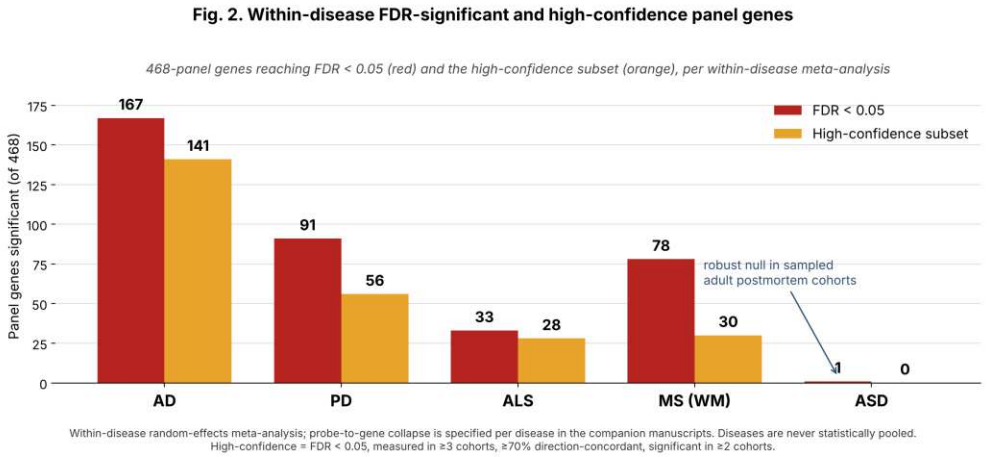


Fig. 2. Within-disease meta-analysis results across adult neurodegenerative diseases and a null ASD adult-brain analysis. Number of 468-panel genes reaching FDR < 0.05 and the high-confidence subset in independent within-disease random-effects meta-analyses: AD, 167/141; PD, 91/56; ALS, 33/28; MS white matter, 78/30; ASD, 1/0. Diseases are analyzed within disease and are never statistically pooled. Counts do not establish preferential enrichment of the full 468-gene panel relative to matched random gene sets. The ASD adult postmortem-brain analysis is a robust null in the sampled cohorts.

Table 1. Published variants in panel genes inventoried in the companion manuscripts. Each entry is a variant or variant–exposure finding, not a distinct gene, and is itemised with its source in the companion table named. No entry was genotyped in the transcriptomic cohorts analysed here. Odds ratios were taken from the cited source studies and were not re-estimated. The multiple sclerosis and ALS companions are transcriptomic analyses and contain no variant inventory. This table is descriptive and does not establish clinical validity of GVI, DDI, IDRS, or any related research construct.

Disease	Entries	Where itemised	Grouping in the source table
AD	10	Alzheimer companion, Table 6	4 eligible for the GVI sum; 5 published AD findings excluded from the sum; 1 with no supporting evidence
PD	10	Parkinson companion, Table 5	Inventory only; not combined into a GVI in the companion; none genotyped in the PD cohorts
ASD	15	Autism companion, Table 8	2 maternal-genotype ASD findings (the maternal GVI sum); 8 child-genotype findings and 5 findings with non-ASD outcomes, given as context
MS	0	—	No variant inventory (transcriptomic companion)
ALS	0	—	No variant inventory (transcriptomic companion)
Total	**35**		

Declaration of generative AI and AI-assisted technologies in the manuscript preparation process

During the preparation of this work the author used Grok (xAI), Claude (Anthropic) and Perplexity to assist with literature synthesis, bioinformatic pipeline construction, editorial refinement, and critical review of claims and citations. After using these tools, the author reviewed and edited the content as needed and takes full responsibility for the content of the published article. No generative tool is an author.

REFERENCES AND NOTES

1. R. G. Roy, P. K. Mandal, J. C. Maroon, Oxidative stress occurs prior to amyloid Aβ plaque formation and tau phosphorylation in Alzheimer's disease: role of glutathione and metal ions. ACS Chem. Neurosci. 14, 2944–2954 (2023). https://doi.org/10.1021/acschemneuro.3c00486

2. V. Mandic-Maravic et al., Glutathione S-transferase polymorphisms and clinical characteristics in autism spectrum disorders. Front. Psychiatry 12, 672389 (2021). https://doi.org/10.3389/fpsyt.2021.672389

3. J. Sian et al., Alterations in glutathione levels in Parkinson's disease and other neurodegenerative disorders affecting basal ganglia. Ann. Neurol. 36, 348–355 (1994). https://doi.org/10.1002/ana.410360305

4. C. Peggion et al., SOD1 in ALS: taking stock in pathogenic mechanisms and the role of glial and muscle cells. Antioxidants (Basel) 11, 614 (2022). https://doi.org/10.3390/antiox11040614

5. R. Gold et al., Clinical use of dimethyl fumarate in multiple sclerosis treatment: an update to include China, using a modified Delphi method. Ther. Adv. Neurol. Disord. 16, 17562864231180734 (2023). https://doi.org/10.1177/17562864231180734

6. M. E. McCaulley, Impaired pathways of detoxification and risk of Alzheimer's disease: Differential gene expression studies via gene set expression analysis. J. Alzheimers Dis. Rep. 10, 25424823261419382 (2026). https://doi.org/10.1177/25424823261419382

7. J. X. Santos et al., A role for gene-environment interactions in autism spectrum disorder is supported by variants in genes regulating the effects of exposure to xenobiotics. Front. Neurosci. 16, 862315 (2022). https://doi.org/10.3389/fnins.2022.862315

8. S. Kant et al., Choroid plexus genes for CSF production and brain homeostasis are altered in Alzheimer's disease. Fluids Barriers CNS 15, 34 (2018). https://doi.org/10.1186/s12987-018-0120-7

9. K. Tachibana et al., Association of plasma claudin-5 with age and Alzheimer disease. Int. J. Mol. Sci. 25, 1419 (2024). https://doi.org/10.3390/ijms25031419

10. F. Verde et al., PON1 is a disease modifier gene in amyotrophic lateral sclerosis: association of the Q192R polymorphism with bulbar onset and reduced survival. Neurol. Sci. 40, 1469–1473 (2019). https://doi.org/10.1007/s10072-019-03834-2

11. P. N. Valdmanis et al., Association of paraoxonase gene cluster polymorphisms with ALS in France, Quebec, and Sweden. Neurology 71, 514–520 (2008). https://doi.org/10.1212/01.wnl.0000324997.21272.0c

12. C. O. Reichert, D. Levy, S. P. Bydlowski, Paraoxonase role in human neurodegenerative diseases. Antioxidants (Basel) 10, 11 (2021). https://doi.org/10.3390/antiox10010011

13. X. Wang et al., STING aggravates ferroptosis-dependent myocardial ischemia-reperfusion injury by targeting GPX4 for autophagic degradation. Signal Transduct. Target. Ther. 10, 136 (2025). https://doi.org/10.1038/s41392-025-02216-9

14. A. S. Ferecskó et al., STING-triggered CNS inflammation in human neurodegenerative diseases. Biomedicines 11, 1375 (2023). https://doi.org/10.3390/biomedicines11051375

15. E. M. Szegő et al., Constitutively active STING causes neuroinflammation and degeneration of dopaminergic neurons in mice. eLife 11, e81943 (2022). https://doi.org/10.7554/eLife.81943

16. H. Akiyama et al., Expression of intercellular adhesion molecule (ICAM)-1 by a subset of astrocytes in Alzheimer disease and some other degenerative neurological disorders. Acta Neuropathol. 85, 628–634 (1993). https://doi.org/10.1007/BF00334673

17. I. Wimmer et al., PECAM-1 stabilizes blood-brain barrier integrity and favors paracellular T-cell diapedesis across the blood-brain barrier during neuroinflammation. Front. Immunol. 10, 711 (2019). https://doi.org/10.3389/fimmu.2019.00711

18. F. Kerr et al., Direct Keap1-Nrf2 disruption as a potential therapeutic target for Alzheimer's disease. PLoS Genet. 13, e1006593 (2017). https://doi.org/10.1371/journal.pgen.1006593

19. S. Davinelli et al., Oxidative stress response and NRF2 signaling pathway in autism spectrum disorder. Redox Biol. 83, 103661 (2025). https://doi.org/10.1016/j.redox.2025.103661

20. M. E. McCaulley, Autism spectrum disorder and mercury toxicity: use of genomic and epigenetic methods to solve the etiologic puzzle. Acta Neurobiol. Exp. (Wars.) 79, 113–125 (2019). https://doi.org/10.21307/ane-2019-010

21. J. Kirby et al., Mutant SOD1 alters the motor neuronal transcriptome: implications for familial ALS. Brain 128, 1686–1706 (2005). https://doi.org/10.1093/brain/awh503

22. R. Gold et al., Placebo-controlled phase 3 study of oral BG-12 for relapsing multiple sclerosis. N. Engl. J. Med. 367, 1098–1107 (2012). https://doi.org/10.1056/NEJMoa1114287

23. S. Gopal et al., Evidence of activation of the Nrf2 pathway in multiple sclerosis patients treated with delayed-release dimethyl fumarate in the phase 3 DEFINE and CONFIRM studies. Mult. Scler. 23, 1875–1883 (2017). https://doi.org/10.1177/1352458517690617

24. G. J. Michael et al., Up-regulation of metallothionein gene expression in parkinsonian astrocytes. Neurogenetics 12, 295–305 (2011). https://doi.org/10.1007/s10048-011-0294-5

25. W. Macnair et al., snRNA-seq stratifies multiple sclerosis patients into distinct white matter glial responses. Neuron 113, 396–410.e9 (2025). https://doi.org/10.1016/j.neuron.2024.11.016

26. M. Ma et al., The spatial landscape of glial pathology and T cell response in Parkinson's disease substantia nigra. Nat. Commun. 16, 7146 (2025). https://doi.org/10.1038/s41467-025-62478-3

27. G. Liu et al., Aldehyde dehydrogenase 1 defines and protects a nigrostriatal dopaminergic neuron subpopulation. J. Clin. Invest. 124, 3032–3046 (2014). https://doi.org/10.1172/JCI72176

28. M. C.-Y. Wey et al., Neurodegeneration and motor dysfunction in mice lacking cytosolic and mitochondrial aldehyde dehydrogenases: implications for Parkinson's disease. PLoS One 7, e31522 (2012). https://doi.org/10.1371/journal.pone.0031522

29. Q. Wang et al., Molecular profiling of human substantia nigra identifies diverse neuron types associated with vulnerability in Parkinson's disease. Sci. Adv. 10, eadi8287 (2024). https://doi.org/10.1126/sciadv.adi8287

30. T. K. Grønborg, D. E. Schendel, E. T. Parner, Recurrence of autism spectrum disorders in full- and half-siblings and trends over time: a population-based cohort study. JAMA Pediatr. 167, 947–953 (2013). https://doi.org/10.1001/jamapediatrics.2013.2259

31. J. J. Goeman, P. Bühlmann, Analyzing gene expression data in terms of gene sets: methodological issues. Bioinformatics 23, 980–987 (2007). https://doi.org/10.1093/bioinformatics/btm051

32. D. Wu, G. K. Smyth, Camera: a competitive gene set test accounting for inter-gene correlation. Nucleic Acids Res. 40, e133 (2012). https://doi.org/10.1093/nar/gks461

Statements and Declarations. Funding: The author declares that no funds, grants, or other support were received during the preparation of this manuscript. All work was conducted independently through Sirius Neuroscience, LLC.

Author contributions: M.E.M. — Conceptualization; Data curation; Formal analysis; Investigation; Methodology; Project administration; Resources; Software; Validation; Visualization; Writing – original draft; Writing – review and editing.

Competing interests: The author is sole inventor on a provisional patent application covering panel-based research scoring methods that use the locked 468-gene list reported here. The application did not determine gene membership, the high-confidence rule, or the results. GVI,

DDI, and IDRS are unvalidated research constructs. Academic reuse of the deposited panel and code does not require a license from the author. The author declares no other competing interests.

Ethics approval: This study used only publicly available, de-identified gene-expression data from NCBI GEO and cited public repositories. No new human participants were recruited. Institutional review board approval was not required. Consent to participate: Informed consent for original sample collection was obtained by the depositing investigators. No additional consent was required for this secondary analysis. Consent to publish: Not applicable (no identifiable individual data). Data and Materials Availability: Transcriptomic analyses use publicly available GEO datasets. The locked 468-gene panel, excluded-symbol list, GEO accession roles, locked per-disease meta counts, methods supplement, and analysis pipeline are deposited at Zenodo under the concept DOI https://doi.org/10.5281/zenodo.22178093; version 1.0 (https://doi.org/10.5281/zenodo.22178094) holds the locked panel and rules, and later versions add the Parkinson per-gene meta-analysis table and the Alzheimer reproduction package. The ALS row of the deposited per-disease meta counts (456 / 26 / 22) is superseded by the donor-resolved analysis reported here (449 / 33 / 28), and the revised cross-disease list is Online Resource 3. Companion manuscripts will cite this article's identifier when available.

Companion manuscripts

AD companion. M. E. McCaulley, A locked 468-gene detoxification panel in Alzheimer's disease brain, liver, and blood: 141 high-confidence cerebral associations including lower CYP46A1 transcript abundance, and a 12-sample hepatic CYP7A1 signal. Research Square, version 1 (2026). https://doi.org/10.21203/rs.3.rs-10999456/v1

ASD companion. M. E. McCaulley, A null adult postmortem-brain test of a locked 468-gene panel in autism spectrum disorder, with published maternal-axis architecture as context. Adult postmortem-brain high-confidence count is zero. Research Square, version 1 (2026). https://doi.org/10.21203/rs.3.rs-11553062/v1

PD companion. M. E. McCaulley, Panel-gene transcriptomic associations and published-variant architecture in Parkinson disease. Research Square, version 1 (2026). https://doi.org/10.21203/rs.3.rs-11097203/v1

MS companion. M. E. McCaulley, Panel-gene transcriptomic associations in multiple sclerosis: a three-cohort white-matter analysis of a locked 468-gene detoxification panel. Research Square, version 1 (2026). https://doi.org/10.21203/rs.3.rs-11530178/v1

ALS companion. M. E. McCaulley, Panel-gene transcriptomic associations in amyotrophic lateral sclerosis: a donor-resolved seven-cohort analysis of a locked 468-gene detoxification panel. Research Square, version 1 (2026). https://doi.org/10.21203/rs.3.rs-11552529/v1

Supplementary Files

This is a list of supplementary files associated with this preprint. Click to download.

- ESM1OnlineResource1notesstatusupdatedv220261119.pdf
- ESM2OnlineResource2TableS0468genepanelREVISED20261003.xlsx
- ESM3OnlineResource3TableS153genesstatusupdated20261119.xlsx